Circulation Research

ORIGINAL RESEARCH

Diminished PLK2 Induces Cardiac Fibrosis and Promotes Atrial Fibrillation

Stephan R. Künzel,* Maximilian Hoffmann,* Silvio Weber, Karolina Künzel, Susanne Kämmerer, Mario Günscht, Erik Klapproth, Johanna S.E. Rausch, Mirna S. Sadek, Tomasz Kolanowski, Stefanie Meyer-Roxlau, Christopher Piorkowski, Sems M. Tugtekin, Stefan Rose-John, Xiaoke Yin, Manuel Mayr, Jan Dominik Kuhlmann, Pauline Wimberger, Konrad Grützmann, Natalie Herzog, Jan-Heiner Küpper, Molly O'Reilly, S. Nashitha Kabir, Laura C. Sommerfeld, Kaomei Guan, Ben Wielockx, Larissa Fabritz, Stanley Nattel, Ursula Ravens, Dobromir Dobrev, Michael Wagner,† Ali El-Armouche†

RATIONALE: Fibrosis promotes the maintenance of atrial fibrillation (AF), making it resistant to therapy. Improved understanding of the molecular mechanisms leading to atrial fibrosis will open new pathways toward effective antifibrotic therapies.

OBJECTIVE: This study aims to decipher the mechanistic interplay between PLK2 (polo-like kinase 2) and the profibrotic cytokine OPN (osteopontin) in the pathogenesis of atrial fibrosis and AF.

METHODS AND RESULTS: Atrial PLK2 mRNA expression was 10-fold higher in human fibroblasts than in cardiomyocytes. Compared with sinus rhythm, right atrial appendages and isolated right atrial fibroblasts from patients with AF showed downregulation of PLK2 mRNA and protein, along with increased PLK2 promotor methylation. Genetic deletion as well as pharmacological inhibition of PLK2 induced profibrotic phenotype conversion in cardiac fibroblasts and led to a striking de novo secretion of OPN. Accordingly, PLK2-deficient (PLK2 knockout) mice showed cardiac fibrosis and were prone to experimentally induced AF. In line with these findings, OPN plasma levels were significantly higher only in patients with AF with atrial low-voltage zones (surrogates of fibrosis) compared with sinus rhythm controls. Mechanistically, we identified ERK1/2 as the relevant downstream mediator of PLK2 leading to increased OPN expression. Finally, oral treatment with the clinically available drug mesalazine, known to inhibit ERK1/2, prevented cardiac OPN overexpression and reversed the pathological PLK2 knockout phenotype in PLK2 knockout mice.

CONCLUSIONS: Abnormal PLK2/ERK1/2/OPN axis function critically contributes to AF-related atrial fibrosis, suggesting reinforcing PLK2 activity and/or OPN inhibition as innovative targets to prevent fibrosis progression in AF. Mesalazine derivatives may be used as lead compounds for the development of novel anti-AF agents targeting fibrosis.

GRAPHIC ABSTRACT: An online graphic abstract is available for this article.

Key Words: atrial fibrillation ■ fibroblasts ■ fibrosis ■ mesalamine ■ osteopontin

Meet the First Author, see p 769

Atrial fibrillation (AF) is a cardiac arrhythmia with rising prevalence that contributes significantly to morbidity and mortality worldwide.[1] Repetitive AF episodes lead to marked changes in cardiac tissue architecture that in turn favor AF recurrence and maintenance.[2–4] Current antiarrhythmic drugs suppress arrhythmic episodes by

Correspondence to: Michael Wagner, MD, Department of Rhythmology, Clinic for Internal Medicine and Cardiology, Herzzentrum Dresden GmbH, Fetscherstraße 76, 01307 Dresden, Germany, Email michael_wagner@tu-dresden.de or Ali El-Armouche, MD, Institute of Pharmacology and Toxicology, Faculty of Medicine Carl Gustav Carus, Technische Universität Dresden, Fetscherstraße 74, 01307 Dresden, Germany, Email ali.el-armouche@tu-dresden.de
*S.R. Künzel and M. Hoffmann contributed equally.
†M. Wagner and A. El-Armouche contributed equally.
The Data Supplement is available with this article at https://www.ahajournals.org/doi/suppl/10.1161/CIRCRESAHA.121.319425.
For Sources of Funding and Disclosures, see page 818.

Novelty and Significance

What Is Known?

- Atrial fibrillation (AF) is the clinically most prevalent cardiac arrhythmia resulting in considerable morbidity and mortality worldwide.
- Recently, the concept of atrial cardiomyopathy has arisen, placing progressive atrial fibrosis in the center of the disease process.
- PLK2 (polo-like kinase 2) is a serine-threonine kinase that regulates cell cycle progression by centriole duplication, and it is strongly associated with cell proliferation, mitochondrial respiration, and apoptosis.

What New Information Does This Article Contribute?

- PLK2 is downregulated in atrial appendages and right atrial fibroblasts from patients with AF.
- Pharmacological as well as genetic deletion (PLK2 KO) of PLK2 results in fibrotic remodeling, susceptibility for AF, and induces de novo expression of OPN (osteopontin); patients with AF with cardiac fibrosis have increased OPN plasma levels.
- Treatment with mesalazine, known to inhibit ERK1/2, prevents cardiac OPN overexpression and the pathological PLK2 KO phenotype.

AF is a cardiac arrhythmia with rising prevalence that contributes significantly to morbidity and mortality worldwide. Repetitive AF episodes lead to marked changes in cardiac tissue architecture that in turn favor AF recurrence and maintenance. Recently, there has been a paradigm shift in the understanding of AF pathophysiology, with awareness of AF involving an atrial cardiomyopathy encompassing progressive fibrosis in many patients. We identify the serine-threonine kinase PLK2 as a key player in atrial fibrosis. Right atrial appendages and isolated right atrial fibroblasts from patients with AF showed downregulation of PLK2, along with increased PLK2 promotor methylation. Genetic deletion as well as pharmacological inhibition of PLK2 induced profibrotic phenotype conversion in cardiac fibroblasts and led to de novo secretion of OPN. PLK2-deficient (PLK2 KO) mice showed cardiac fibrosis and were prone to experimental AF. In line with these findings, OPN plasma levels were significantly higher only in patients with AF with atrial low-voltage zones (surrogates of fibrosis) compared with SR controls. Finally, oral treatment with mesalazine prevented cardiac OPN overexpression and the pathological PLK2 KO phenotype. Consequently, we identify the PLK2/OPN axis as a target to counter atrial fibrosis in AF to prevent disease progression.

Nonstandard Abbreviations and Acronyms

αSMA	alpha smooth muscle actin
AF	atrial fibrillation
DNMT	DNA-methyl-transferase
FAPα	fibroblast activation protein alpha
FIH-1	factor-inhibiting HIF
HAF	human atrial fibroblast
HIF-1α	hypoxia-inducible factor
OPN	osteopontin
PHF	PHD finger protein
PLK2	polo-like kinase 2
SR	sinus rhythm
WT	wild type

preferentially blocking cardiac ion channels. However, in a large proportion of patients, these approaches are insufficient and may produce detrimental side effects including proarrhythmia and extracardiac toxicity.[5,6] Recently, there has been a paradigm shift in the understanding of AF pathophysiology, with awareness of AF involving an atrial cardiomyopathy encompassing progressive fibrosis in many patients.[1,7] Any kind of cardiac injury or disorder that activates fibroblasts leads to differentiation to more active myofibroblasts.[8,9] Myofibroblasts reduce their proliferative activity, gain size, express orderly arranged filaments of αSMA (alpha smooth muscle actin), and become highly secretory, resulting in the deposition of interstitial collagen and other matrix proteins as well as local enrichment of cytokines.[8,10] We have recently provided evidence for altered fibroblast function in patients with persistent AF in terms of increased myofibroblast differentiation and reduced in vitro fibroblast proliferation.[11] However, the underlying molecular mechanisms remain widely elusive.

We previously focused on differentially regulated genes in fibroblasts isolated from patients with persistent AF. An Affymetrix microarray revealed negative regulation of PLK2 (polo-like kinase 2) transcripts in AF.[11] PLK2 is a serine-threonine kinase that regulates cell cycle progression by centriole duplication, and it is strongly associated with cell proliferation, mitochondrial respiration, and apoptosis.[12–14] However, its role in heart disease is poorly defined. The objective of the present study was to clarify the pathophysiological role of PLK2 in atrial fibrosis and the pathogenesis of AF and to identify PLK2-dependent

target proteins. We provide evidence linking a reduction in PLK2 expression, in patients, as well as in experimental AF, to increased ERK1/2 phosphorylation and subsequent secretion of OPN (osteopontin), a cytokine-like glycoprotein of the extracellular matrix critically involved in cardiac fibrosis and remodeling.[15–23] Moreover, we demonstrate prevention of the profibrotic PLK2 knockout phenotype by long-term oral application of the clinically approved drug mesalazine (5-aminosalicylic acid) known to inhibit the ERK/OPN axis.[24]

METHODS

Data Availability

The authors declare that all supporting data are available within the article and its Data Supplement.

A detailed, expanded Methods section is provided in the Data Supplement. Please, see the Major Resources Table in the Data Supplement.

Study Approval

All patients participating in this study gave written informed consent according to the Declaration of Helsinki, and the study was approved by the institutional review committee (Official file numbers: EK 114082202, EK 465122013). The Institutional Animal Care and Use Committee at Technische Universität Dresden approved all animal experiments (Official file numbers: T 2014/5, TVA 25/2017, TVV 64/2018). All experiments at the University of Birmingham were conducted according to the Animals (Scientific Procedures) Act 1986 and approved by the Home Office (Home Office References 30/2967 and the institutional review board at the University of Birmingham, United Kingdom. Animal experiments were planned as pilot study without a priory power calculation in accordance with the Institutional Animal Care and Use Committee.

Statistical Analysis

Results are presented as mean±SEM. For statistical analysis and graphic representation of the data, Graph Pad Prism software v.8 (GraphPad Software, San Diego) was used. All data were tested for normality with the Kolmogorov-Smirnov test. A nonparametric test was used when data were not normally distributed or sample size was below 6. For comparisons between 2 groups only, Student *t* test for normally distributed data or Mann-Whitney *U* test for non-normally distributed data were used. When comparing 3 groups, 1-way ANOVA or Kruskal-Wallis test were performed with Tukey or Dunn post-test, respectively. Categorical data were analyzed with χ^2 test. Ca^{2+} imaging data and the histological sections of the mesalazine study were analyzed using a hierarchical model in R using the lme4 package with clustering for the individual mice as described previously.[25] Proteomics data were filtered for missing values, logarithmized, and statistical significance was calculated with Bayesian statistics using the ebayes function of the limma package in R. Final *P* values were corrected for multiple testing using the Benjamini Hockberg method. Statistical tests and corresponding post-tests are indicated in the respective figure legends. Relative values are expressed in relation to the corresponding control values. A 2-tailed $P<0.05$ was considered statistically significant.

Units and Relative Expression

Whenever possible, SI units were used throughout the entire article. In case of a unit-less result, the term arbitrary unit was used. Relative values are expressed in relation to the corresponding housekeeping gene or protein and subsequently to the according control values.

RESULTS

PLK2 Expression Is Reduced in AF

PLK2 protein abundance was downregulated by ≈50% in right atrial appendages from patients suffering from AF compared with sinus rhythm (SR; $P=7.28\times10^{-3}$, Figure 1A, for patient characteristics see Table IV in the Data Supplement). In patient-derived atrial fibroblasts, *PLK2* expression was 10-fold higher than in atrial cardiomyocytes ($P=4.58\times10^{-4}$, Figure 1B). *PLK2* mRNA expression was lower in primary outgrowth atrial fibroblasts of AF compared with patients with SR (Figure 1B, for patient characteristics, see Table II in the Data Supplement). The reduction of PLK2 was associated with an increase in fibrotic marker proteins FAPα (fibroblast activation protein alpha), αSMA, and vimentin in right atrial appendages from patients with AF compared with SR (Figure 1C through 1E). Last, we validated our findings in an established dog model of atrial fibrosis-associated AF due to ventricular tachycardiomyopathy.[26] After 2 weeks of ventricular tachypacing-induced remodeling, we detected significantly lower PLK2 expression (≈50%) in atrial tissue ($P=2.53\times10^{-3}$, Figure 1F).

Long-Term Regulation of PLK2 by Promotor Methylation

Previous studies in noncardiac tissues[27,28] have shown that PLK2 expression is strongly regulated by promoter hypermethylation. Therefore, we performed methylation-specific PCR for the *PLK2* promoter, which was positive in 6 out of 13 AF samples, while there was no detectable methylation of the *PLK2* promoter in any of the SR samples (n=11, $P=9.27\times10^{-3}$, Figure 2A; Table XII in the Data Supplement). The smoking status of the patients did not significantly correlate with the presence or absence of promoter methylation (Figure V and Table XIII in the Data Supplement). To test the hypothesis that *PLK2* is regulated by promotor methylation in atrial fibroblasts, we exposed human atrial fibroblasts of a recently established human atrial fibroblast (HAF) cell line (HAF-SRK01)[29] to chronic hypoxia (1% O_2) exposure for 24 and 96 hours (Figure 2B through 2G), because hypoxia has been shown to induce PLK2 promotor methylation in lymphocytes[27] and tissue hypoxia occurs during AF.[30,31]

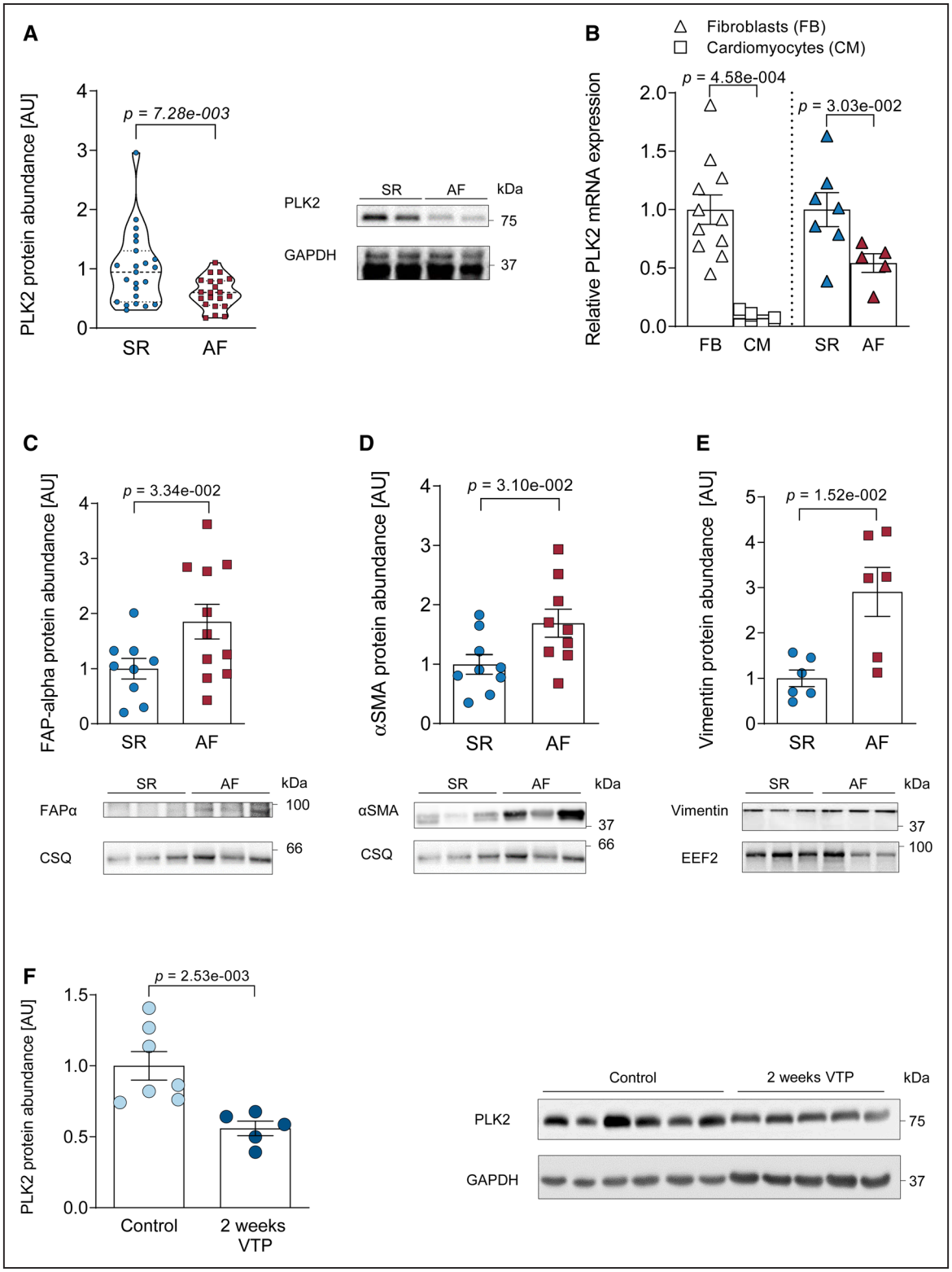

Figure 1. PLK2 (polo-like kinase 2) expression is reduced in clinical as well as experimentally induced atrial fibrillation (AF) and myofibroblast markers are concomitantly increased.

A, Quantification of PLK2 protein abundance in human right atrial tissue from sinus rhythm (SR) and patients with AF, normalized to GAPDH (SR [n=23], AF [n=21]; results are given as mean±SEM determined by a Welch *t* test). **B**, Left, expression of *PLK2* mRNA (qPCR) normalized to *GAPDH* as housekeeping gene in primary human atrial fibroblasts vs cardiomyocytes from patients with SR. Right, mRNA levels of PLK2 normalized to *GAPDH* as housekeeping gene in human atrial fibroblasts from patients with SR and AF (FB [n=11], CM [n=5], SR [n=7], AF [n=5]; results are given as mean±SEM, *P* value was determined by a Mann-Whitney *U* test). **C**, Whole-tissue protein abundance of FAPα (fibroblast activation protein alpha) in SR and AF, normalized to calsequestrin (CSQ) (SR [n=9], AF [n=11]; results are given as mean±SEM, (*Continued*)

Within 24 hours, we found a 3.2-fold downregulation of *PLK2* mRNA expression (P=1.13×10^{-3}, Figure 2B). Methylation of the *PLK2* promoter was detectable only after 96 hours exposure to chronic hypoxia (Figure 2C). PLK2 protein was strongly reduced within 24 hours of hypoxia (P=9.52×10^{-3}, Figure 2D, left) and almost abolished after 96 hours of hypoxia (P=9.52×10^{-3}, Figure 2D, right). As a positive control, cells were treated with 0.25 mmol/L dimethyloxaloylglycine, which mimics hypoxia by upregulation of HIF-1α (hypoxia-inducible factor) with inhibition of PHF (PHD finger protein) and FIH-1 (factor-inhibiting HIF).[32] Dimethyloxaloylglycine treatment for 96 hours led to marked PLK2 promoter methylation (Figure 2C), validating *PLK2* promotor methylation as 1 factor contributing to long-term downregulation of PLK2. Next, we analyzed the expression of DNMTs (DNA-methyl-transferases)[33] after 24 hours of hypoxia and found *DNMT1* and *DNMT3A* being significantly upregulated compared with normoxia control (P=1.83×10^{-6}, Figure 2E and 2F). Accordingly, inhibition of DNA methylation by 5-azacytidine[34] abolished the reduction in PLK2 expression during hypoxia (Figure 2G).

Loss of PLK2 Function Induces Myofibroblast Differentiation and Collagen Deposition

Next, we studied the effects of pharmacological PLK2 inhibition (TC-S 7005, 100 nmol/L, 72 hours) in HAF fibroblasts[29] and the consequences of homozygous genetic PLK2 deletion (PLK2-deficient mice).[35] TC-S 7005 and PLK2 deficiency promoted myofibroblast differentiation as indicated by changes in morphology and expression of αSMA (Figure 3A and 3C), with corresponding reduction of fibroblast proliferation rates (Figure 3B and 3D). In line with the observed phenotype conversion, pharmacological PLK2 inhibition with 100 nmol/L TC-S 7005 for 72 hours led to significantly increased extracellular collagen 1 deposition by HAF fibroblasts (P=3.17×10^{-2}, Figure 3E).

Loss of PLK2 Promotes De Novo Secretion of Osteopontin

Based on the finding that PLK2 inhibition as well as knockout initiated myofibroblast differentiation, we studied the secretory phenotype of PLK2 knockout fibroblasts using mass spectrometry secretome analysis of the cell culture media.[36] Strikingly, we found de novo secretion of OPN in PLK2 knockout fibroblasts (P=2.13×10^{-2}, Figure 4A; a list of all significantly regulated proteins is given in Table VII in the Data Supplement). We then validated the causal relationship between PLK2 and OPN in HAF. PLK2 inhibition with TC-s 7005 for 72 hours led to an increase in OPN protein expression (P=2.25×10^{-2} at 100 nmol/L PLK2i, Figure 4B). Notably, OPN was also elevated in right atrial appendages from patients with AF compared with SR (P=2.96×10^{-2}, Figure 4C). We then assessed the levels of OPN in the peripheral blood of patients with AF undergoing pulmonary vein isolation. To test if the severity of fibrosis in patients with AF is correlated with serum OPN levels, we selected patients with AF with and without low-voltage zones in the left atrium described during their electrophysiological study. Low-voltage zones constitute the electrophysiological surrogate of atrial fibrosis.[37,38] Only in the AF group with low-voltage zone, we detected a significant increase in OPN compared with control (P=1.88×10^{-3}, Figure 4D, patient characteristics are given in Table VI in the Data Supplement). Moreover, when we applied recombinant OPN at 25 ng/mL for 72 hours, we detected a nearly 4-fold increase in αSMA expression in HAF, indicating that OPN acts as a paracrine factor promoting myofibroblast differentiation (P=2.86×10^{-2}, Figure 4E). Finally, hypoxia induced a marked increase in OPN expression in human atrial fibroblasts after 24 hours (P=1.08×10^{-3}), which remained somewhat elevated at 96 hours (P=8.5×10^{-2}, Figure 4F).

Loss of PLK2 Activates the ERK1/2 Pathway to Increase OPN Expression

To establish a mechanistic link between reduced PLK2 expression and increased OPN secretion of atrial fibroblasts, we examined the ERK1/2 pathway, which was shown to act downstream of PLK2 but upstream of OPN.[39,40] We found a 5-fold increase in EKR1/2 phosphorylation in right atrial appendages of patients with AF compared with SR (P=7.83×10^{-3}, Figure 5A). Accordingly, cardiac fibroblasts from PLK2-deficient mice also showed an increase in ERK1/2 phosphorylation (P=2.86×10^{-2}, Figure 5B). Moreover, inhibition of PLK2 with 50 and 100 nmol/L of TC-S 7005 both increased ERK1/2 phosphorylation by 7- to 10-fold, respectively (P=3.41×10^{-2} for 100 nmol/L, Figure 5C). Finally, the OPN overexpression in cardiac PLK2 knockout

Figure 1 Continued. *P* value was determined by an unpaired, 2-tailed *t* test). **D**, Protein abundance of the myofibroblast marker protein αSMA (alpha smooth muscle actin) in whole tissue from SR and AF, normalized to CSQ (SR [n=9], AF [n=9]; results are given as mean±SEM, *P* value was determined by an unpaired, 2-tailed *t* test). **E**, Protein abundance of the fibroblast marker vimentin in SR and AF atria, normalized to EEF2 (eukaryotic-elongation-factor-2; SR [n=6], AF [n=6]; results are given as mean±SEM, *P* value was determined by a Welch test). **F**, Quantification of atrial PLK2 protein abundance in a canine model with increased susceptibility to AF (ventricular tachypacing-induced heart failure) at baseline (control) and after 2 wks of tachypacing (control [n=7], ventricular tachypacing [VTP; n=5]; results are given as mean±SEM, *P* value was determined by a Mann-Whitney *U* test). AU indicates arbitrary unit—relative protein expression normalized to the indicated housekeeping protein and the respective control group.

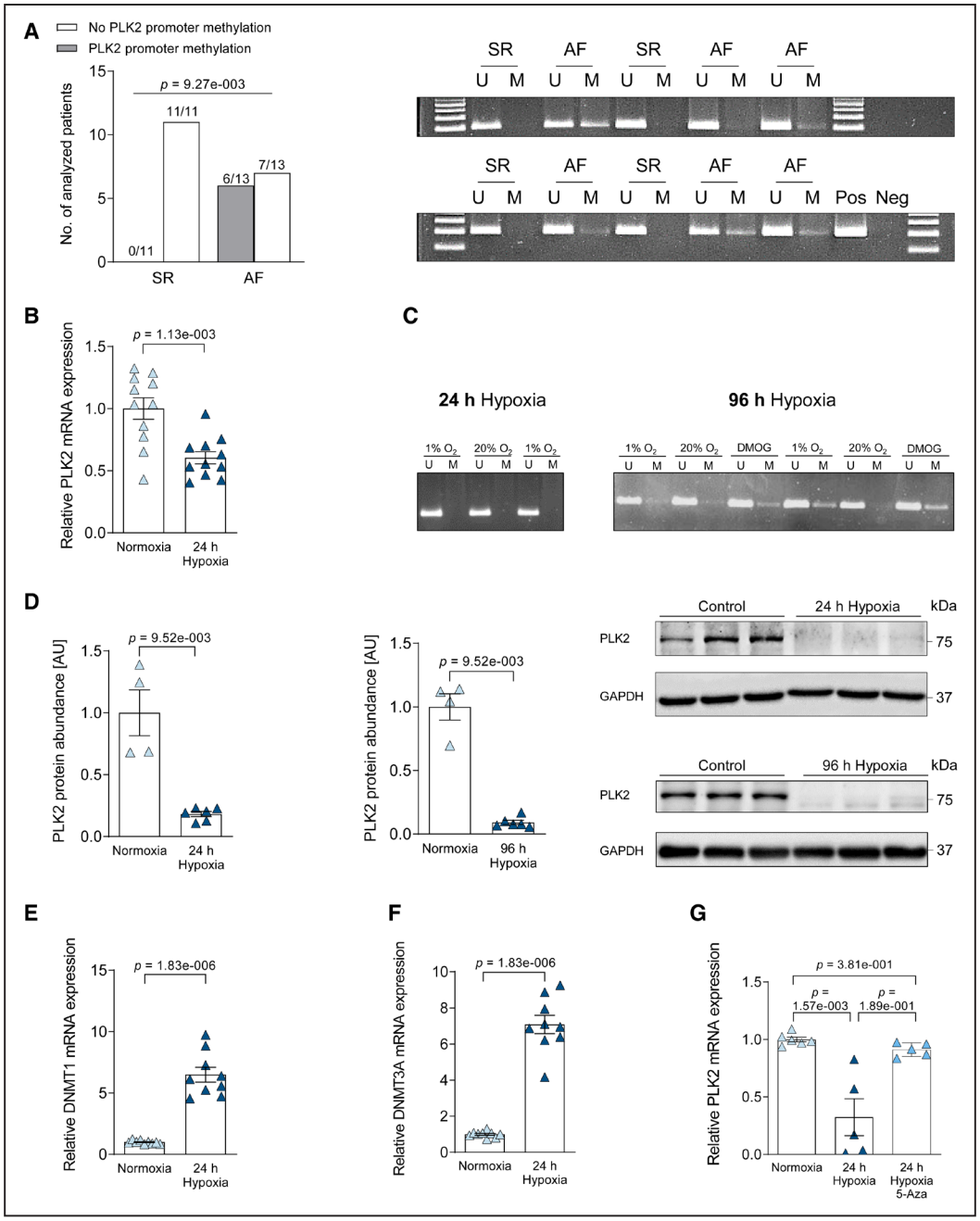

Figure 2. Analysis of the *PLK2* promoter methylation status and hypoxia sensitivity of *PLK2* expression.
A, Quantification of sinus rhythm (SR) and atrial fibrillation (AF) heart tissue samples in which methylation was present or absent. Statistical analysis was done with χ^2 test (SR [n=11], AF [n=13]) and gel images of a methylation-specific PCR of the *PLK2* promotor region (U: unmethylated, M: methylated, Pos: positive control [human universal methylated DNA standard], Neg: water control). **B**, Twenty-four hour hypoxia-dependent (1% O_2) expression of *PLK2* mRNA normalized to *HPRT* as housekeeping gene in human atrial fibroblasts, analyzed by qPCR (control [n=6], hypoxia [n=6]; results are given as mean±SEM, *P* value was determined by a Welch test). **C**, Gel images of a methylation-specific PCR of the *PLK2* promotor region after 24 and 96 h of hypoxia treatment. Dimethyloxaloylglycine (DMOG) treatment for 96 h was used as a positive control (U: unmethylated, M: methylated, Pos: positive control [human universal methylated DNA standard], Neg: water control). **D**, Quantification and representative western blot for PLK2 (polo-like kinase 2) protein expression in human atrial fibroblasts after 24 and 96 h hypoxia treatment (Control [n=4], 24 h hypoxia [n=6], 96 h hypoxia [n=6]; results are given as mean±SEM, *P* value was determined by a Mann-Whitney *U* test). **E**, Twenty-four-hour hypoxia-dependent (1% O_2) expression of *DNMT1* mRNA normalized to *HPRT* as housekeeping gene in human atrial fibroblasts, analyzed by qPCR (control [n=9], hypoxia [n=9]; results are given as mean±SEM, *P* value was determined by a Welch test). **F**, Twenty-four hour hypoxia-dependent (1% O_2) expression of *DNMT3A* mRNA normalized to *HPRT* as housekeeping gene in human atrial fibroblasts, analyzed by qPCR (control [n=9], hypoxia [n=9]; results are given as mean±SEM, *P* value was determined by a Welch test). **G**, The effect of the demethylating drug 5-azacytidine (5-Aza) (10 µmol/L) was evaluated during 24 h hypoxia (1% O_2) treatment. *PLK2* mRNA expression was normalized to *HPRT* as housekeeping gene in human atrial fibroblasts (control [n=6], hypoxia [n=5], hypoxia/5-AZA [n=5]; results are given as mean±SEM, *P* value was determined by a Kruskal-Wallis test with Dunn multiple comparisons test). AU indicates arbitrary unit—relative protein expression normalized to the indicated housekeeping protein and the respective control group.

ORIGINAL RESEARCH

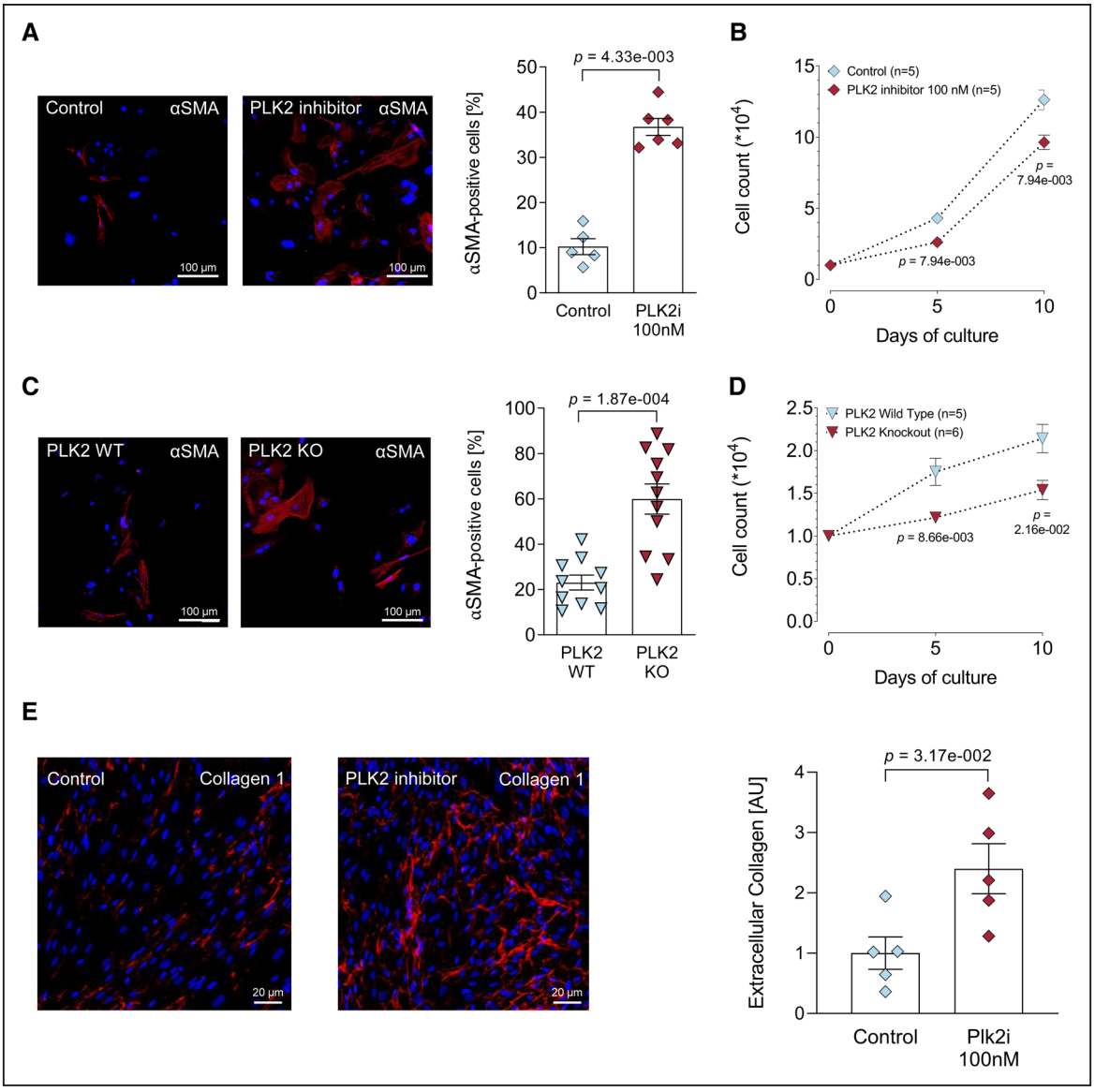

Figure 3. Loss of PLK2 (polo-like kinase 2) function induces a pronounced myofibroblast phenotype.
A, Immunofluorescence images and quantification of αSMA (alpha smooth muscle actin; red) in human atrial fibroblast (HAF)-SRK01 fibroblasts upon PLK2 inhibition with either 100 nmol/L TC-S 7005 or vehicle (1 µL DMSO/mL medium) for 7 d, the nuclei were stained with DAPI (blue) (control [n=5], PLK2i [n=6]; results are given as mean±SEM, *P* value was determined by a Mann-Whitney *U* test). **B**, Proliferation curves of HAF-SRK01 fibroblasts upon PLK2 inhibition with 100 nmol/L TC-S 7005 or vehicle (1 µL DMSO/mL medium; control [n=5], PLK2i [n=5]; results are given as mean±SEM, *P* value was determined by a Mann-Whitney *U* test for each time point). **C**, Immunofluorescence images and quantification of αSMA in PLK2 WT and KO fibroblasts. Primary PLK2 WT and KO fibroblasts were cultivated for 7 d (WT [n=10], knockout [KO; n=11]; results are given as mean±SEM, *P* value was determined by a Welch test). **D**, Proliferation curves of primary PLK2 WT and KO fibroblasts (WT [n=5], KO [n=6]; results are given as mean±SEM determined by a Mann-Whitney *U* test for each time point). **E**, Representative fluorescence images and quantification of extracellular collagen 1 (red) deposition in HAF-SRK01 fibroblasts. The nuclei were stained with DAPI (blue; control [n=5], PLK2i [n=5]; results are given as mean±SEM, *P* value was determined by a Mann-Whitney *U* test). AU indicates arbitrary unit—red (collagen) area normalized to the total nuclear area (blue) of the respective section and subsequently normalized to control.

fibroblasts was absent after specific ERK1/2 inhibition with SCH772984 for 72 hours (P=1.15×10^{-3}, Figure 5D) indicating a causal relationship.

Loss of PLK2 Leads to Left Atrial Dilatation

To assess the functional consequences of PLK2 deficiency, we performed transthoracic echocardiography at the age of 8 months in the PLK2-deficient mice. Left atrial dilatation is a hallmark of clinical AF.[1] Figure 6A depicts representative parasternal long-axis views (left) and M-mode views obtained at the level of the aortic valve (right) recorded from a littermate control (upper) and a PLK2-deficient mouse (lower). Left atrium area was significantly increased both at atrial diastole (P=8.34×10^{-3}, Figure 6B) and in atrial systole

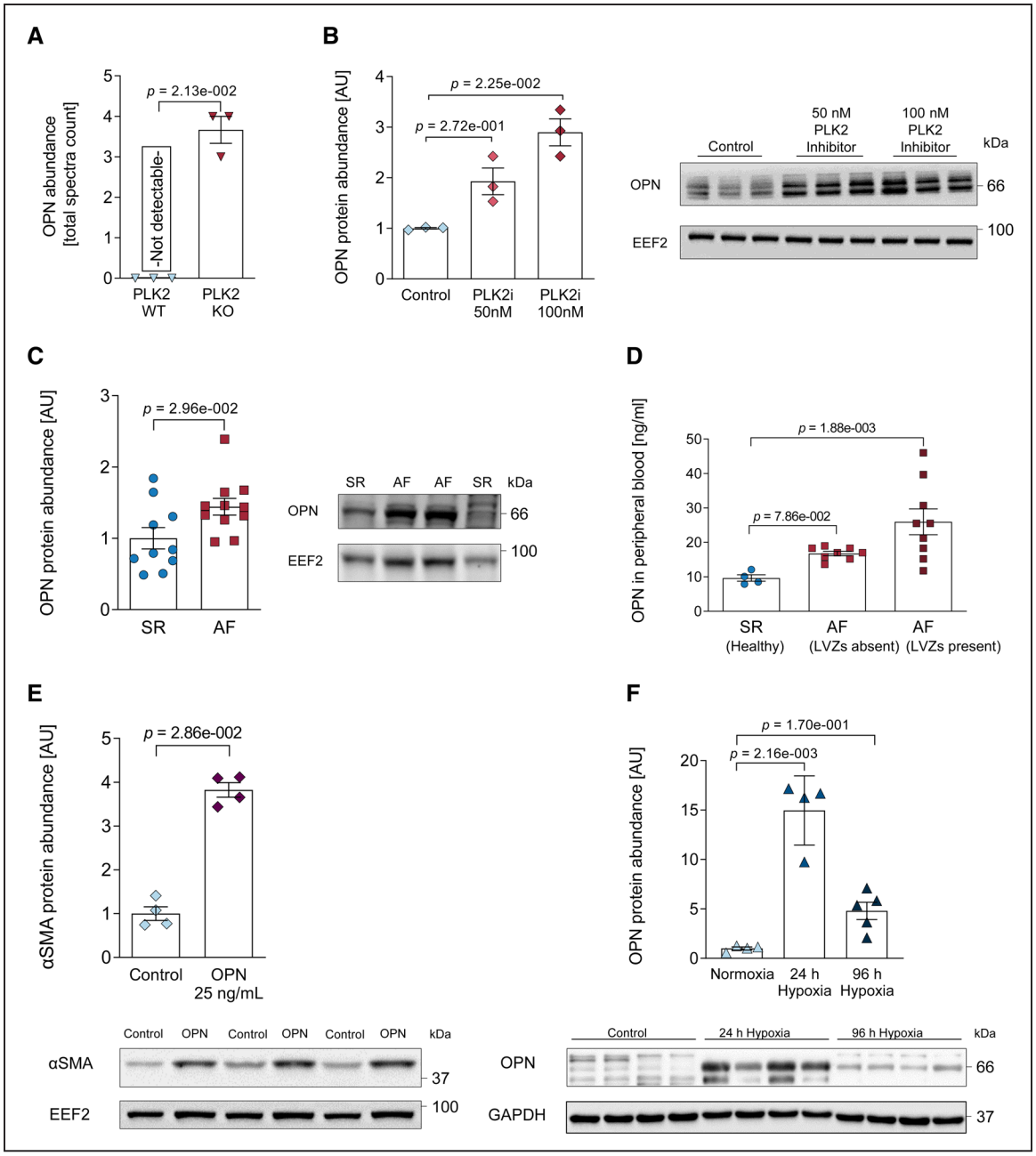

Figure 4. PLK2 (polo-like kinase 2)-dependent osteopontin expression.
A, OPN (osteopontin) protein abundance in PLK2 WT and knockout (KO) primary fibroblast cell culture medium determined by mass spectrometry (WT [n=3], KO [n=3]; results are given as mean±SEM, *P* value was determined by the Benjamini Hockberg method after Bayesian statistics [see Methods]). **B**, Quantification and representative western blot for OPN in human atrial fibroblast (HAF)-SRK01 fibroblasts upon PLK2 inhibition with 50 and 100 nmol/L of the specific PLK2 inhibitor TC-S 7005 (control [n=3], 50 nmol/L [n=3], 100 nmol/L [n=3]; results are given as mean±SEM, *P* value was determined by a Kruskal-Wallis test with Dunn posttest). **C**, Quantification and representative western blot for OPN in sinus rhythm (SR) and atrial fibrillation (AF) right atrial tissue (SR [n=10], AF [n=11]; results are given as mean±SEM, *P* value was determined by an unpaired, 2-tailed *t* test). **D**, ELISA measurement of OPN concentration in the peripheral blood (PB) of healthy control patients in patients with SR and AF with or without electrophysiologically determined low-voltage zones (LVZs) as fibrosis surrogates (SR [n=4], $AF_{LVZ\ absent}$ [n=8], $AF_{LVZ\ present}$ [n=9]; results are given as mean±SEM, *P* value was determined by a Kruskal-Wallis test with Dunn posttest). **E**, Quantification and representative western blot for αSMA (alpha smooth muscle actin) in HAF-SRK01 fibroblasts treated with 25 ng/mL OPN for 72 h (control [n=4], OPN [n=4]; results are given as mean±SEM, *P* value was determined by a Mann-Whitney *U* test). **F**, Quantification and original western blot for OPN protein abundance in HAF-SRK01 fibroblasts after 24 and 96 h hypoxia treatment (control [n=4], 24 h hypoxia [n=5], 96 h hypoxia [n=5]; results are given as mean±SEM, *P* value was determined by a Kruskal-Wallis test with Dunn multiple comparisons test). AU indicates arbitrary unit—relative protein expression normalized to the indicated housekeeping protein and the respective control group.

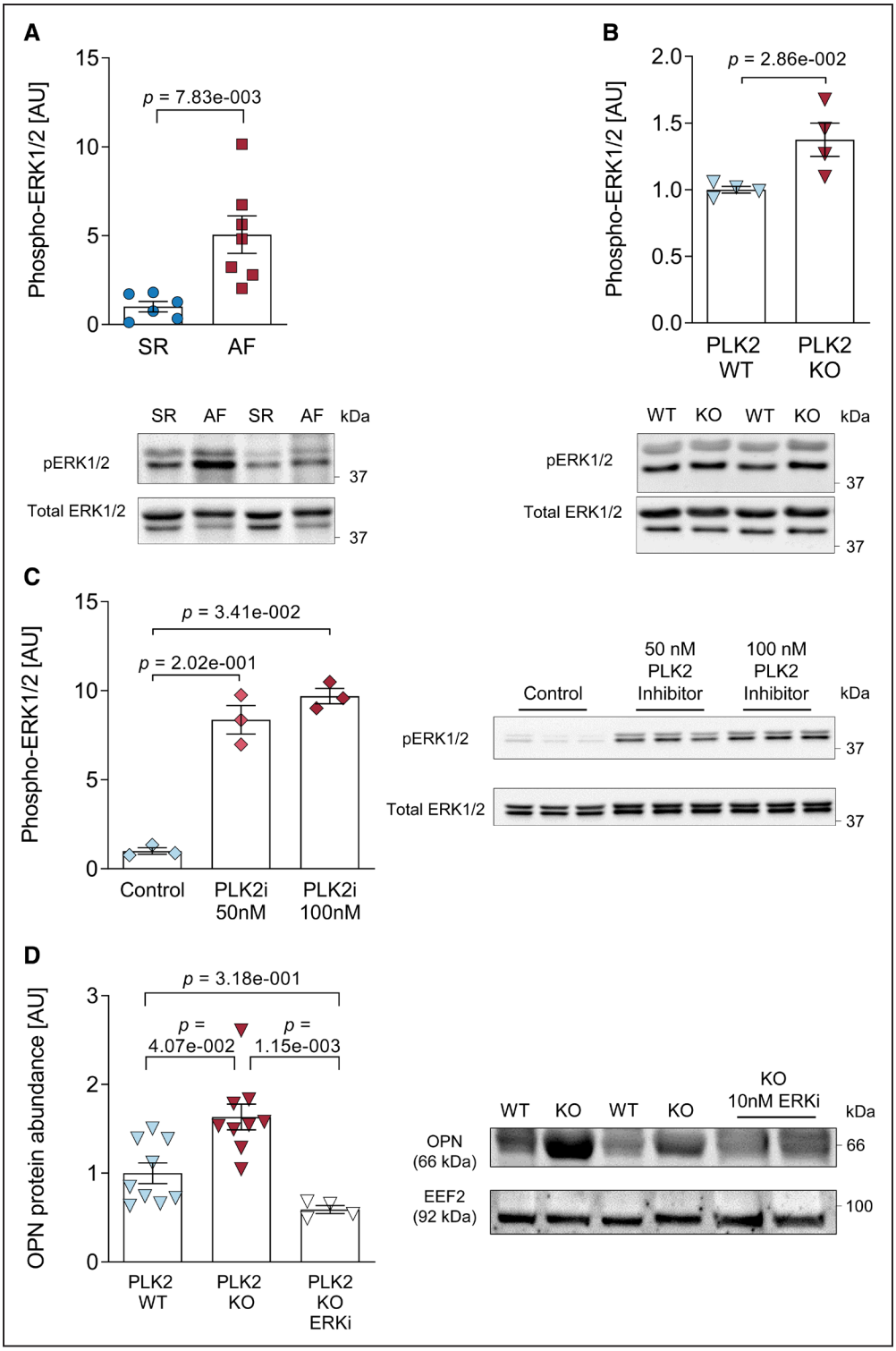

Figure 5. ERK1/2 (extracellular-signal regulated kinases 1/2) phosphorylation and OPN (osteopontin) expression. **A**, Quantification of ERK1/2 phosphorylation and representative western blots in sinus rhythm (SR) tissue samples compared with atrial fibrillation (AF; SR [n=6], AF [n=7]; results are given as mean±SEM, *P* value was determined by a Welch test). **B**, Quantification and representative western blots for ERK1/2 phosphorylation in PLK WT and knockout (KO) primary cardiac fibroblasts (WT [n=4], KO [n=4]; results are given as mean±SEM determined by a Mann-Whitney *U* test). **C**, Quantification and representative western blots for ERK1/2 phosphorylation in human atrial fibroblast (HAF)-SRK01 fibroblasts upon PLK2 inhibition with 50 and 100 nmol/L of the specific PLK2 inhibitor TC-S 7005 (control [n=3], 50 nmol/L [n=3], 100 nmol/L [n=3]; results are given as mean±SEM, *P* value was determined by a Kruskal-Wallis test with Dunn multiple comparison test). **D**, Quantification of OPN protein abundance and representative western blots in primary cardiac PLK2 WT and KO fibroblasts. The specific ERK1/2 inhibitor SCH772984 was used at 10 nmol/L for 72 h (WT [n=9], 50 KO [n=9], KO+ERKi [n=4]; results are given as mean±SEM, *P* value was determined by a Kruskal-Wallis test with Dunn multiple comparisons test). AU indicates arbitrary unit—relative protein expression normalized to the indicated housekeeping protein and the respective control group.

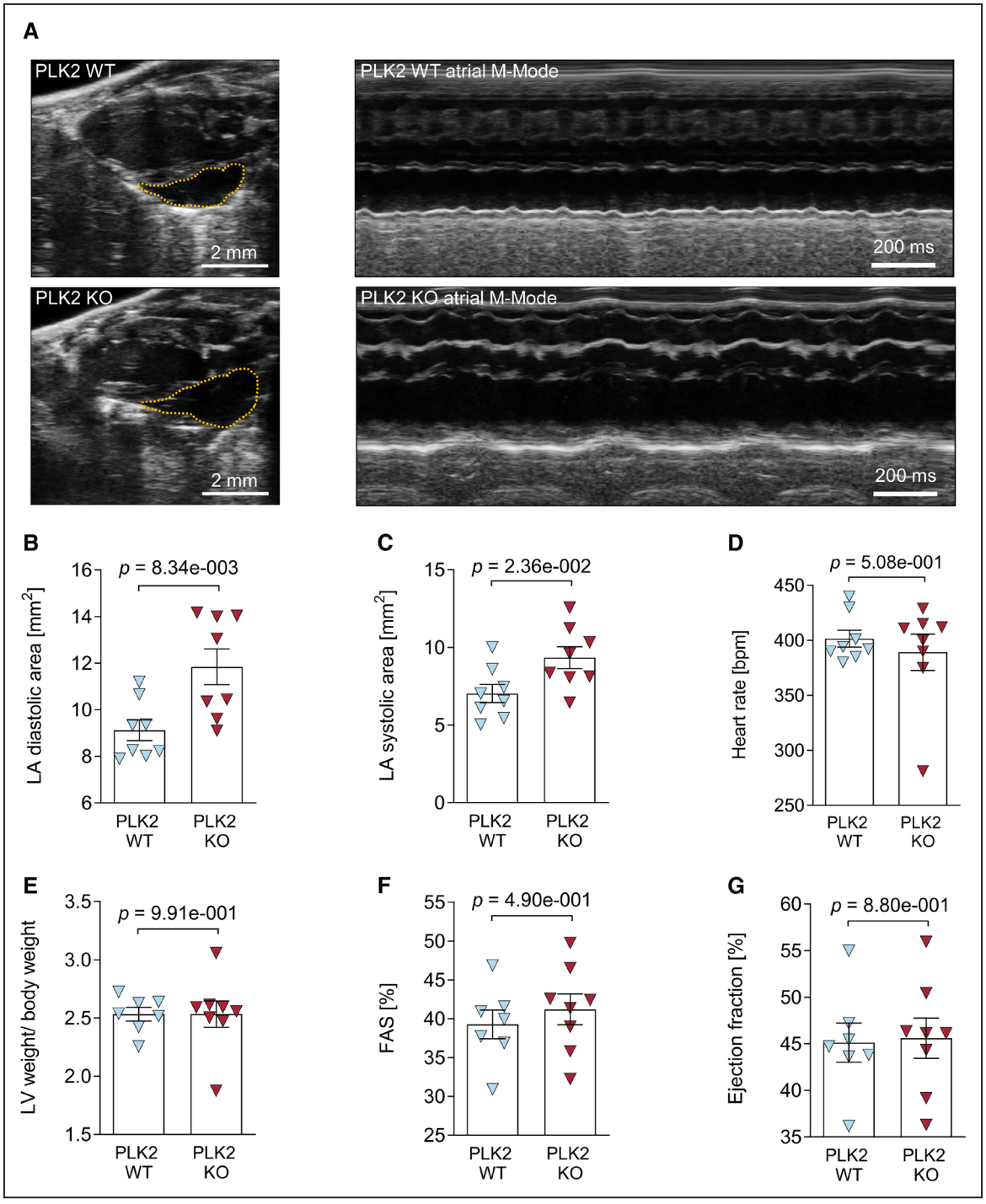

Figure 6. Echocardiographic characterization of PLK2 (polo-like kinase 2)-deficient mice.
Transthoracic echocardiography was performed on isoflurane-anesthetized 8-mo-old PLK2 WT and knockout (KO) mice with a Vevo3100 small animal ultrasound device. **A**, Representative parasternal long-axis views (left) and M-mode views obtained at the level of the aortic valve (right) recorded from a littermate control (PLK2 WT, upper) and a PLK2-deficient mouse (PLK2 KO, lower); **B**, Left atrial diastolic area (WT [n=8], KO [n=8]; results are given as mean±SEM, *P* value was determined by an unpaired, 2-tailed *t* test). **C**, Left atrial systolic area (WT [n=8], KO [n=8]; results are given as mean±SEM, *P* value was determined by an unpaired, 2-tailed *t* test). **D**, Heart rate (WT [n=8], KO [n=8]; results are given as mean±SEM, *P* value was determined by an unpaired, 2-tailed *t* test). **E**, Left ventricular weight to body weight ratio (WT [n=7], KO [n=8]; results are given as mean±SEM, *P* value was determined by a Mann-Whitney *U* test). **F**, Fractional area shortening (WT [n=7], KO [n=8]; results are given as mean±SEM, *P* value was determined by an unpaired, 2-tailed *t* test). **G**, Ejection fraction (WT [n=7], KO [n=7]; results are given as mean±SEM, *P* value was determined by an unpaired, 2-tailed *t* test).

(P=2.36×10^{-2}, Figure 6C) in the PLK2-deficient mice. Heart rate, relative left ventricular weight, and left ventricular fractional area shortening as well as ejection fraction were unaffected (Figure 6D through 6G). A complete list of echocardiographic parameters is given in Table VIII in the Data Supplement.

Loss of PLK2 Causes Interstitial Fibrosis and Increases the Susceptibility to AF

Next, we investigated the presence of interstitial fibrosis in PLK2 knockout whole heart. Figure 7A shows representative Picrosirius red stained paraffin sections of hearts of 8-month-old wild-type (WT) and PLK2 knockout mice cut along the long and short axes. The hearts of the PLK2 knockout mice show marked interstitial, focal, and perivascular fibrosis in the ventricles as well as interstitial fibrosis in the atria. Total ventricular, perivascular, and total atrial fibrosis were increased in PLK2 knockout mice compared with WT littermates ($P=1.73\times10^{-2}$ for total ventricular, $P=4.32\times10^{-4}$ for ventricular perivascular fibrosis, and $P=7.83\times10^{-3}$ for atrial fibrosis; Figure 7A top right panel). At 4 months, fibrosis did not differ between PLK2 knockout and WT mice (Figure I in the Data Supplement). The impact of structural remodeling on the susceptibility toward arrhythmia can be studied using programmed atrial pacing in vivo or ex vivo with Langendorff-perfused hearts. Here, we chose the isolated beating heart model from 8-month-old PLK2-deficient mice and WT littermates using S1 and S1S2 pacing protocols because this model ensures constant coronary perfusion and arrhythmias can be induced several times within the same animal without ischemia. While atrial extrasystoles and short atrial runs were induced by the pacing protocol equally in both groups (WT, 7/9; PLK knockout, 7/9), sustained atrial arrhythmias of >5 fast consecutive extrabeats in a row mimicking AF were induced in 4 out of 9 PKL2 knockout, but in none of 9 WT hearts ($P=2.33\times10^{-2}$, Figure 7B; Table XIV in the Data Supplement). We analyzed action potential duration and atrial effective refractory periods in Langendorff-perfused hearts as well as the expression of Ca^{2+}-handling proteins and Ca^{2+} dynamics. There were no significant differences in expression of Ca^{2+}-handling proteins, properties of Ca^{2+}-transients, atrial action potential duration, or atrial effective refractory periods between PLK2 WT and knockout mice (Figures II through IV in the Data Supplement), pointing to atrial fibrosis as the major determinant of PLK2-mediated arrhythmogenesis.

Long-Term Oral Treatment With Mesalazine Prevents the Fibrotic PLK2 Knockout Phenotype

Finally, we performed a proof-of-concept study with mesalazine (5-aminosalicylic acid), which is approved for inflammatory bowel disease and has been shown to potently inhibit the ERK1/2/OPN axis.[24,41] Starting at 1 month of age, male and female PLK2 knockout mice were orally treated with 100 µg/g mesalazine in the drinking water. After 6 months of treatment, in vivo echocardiography demonstrated suppression of PLK2 knockout-induced left atrial diastolic dilation ($P=1.07\times10^{-2}$) and the trend to systolic atrial dilation ($P=6.779\times10^{-2}$, Figure 8A through 8C). Heart rate and ejection fraction remained unaltered (Figure 8D and 8E). A complete list of echocardiographic parameters is provided in Table IX in the Data Supplement. At the molecular level, mesalazine treatment prevented the increase in *OPN* mRNA expression caused by PLK2 knockout (Figure 8F). Finally, Picrosirius red staining of paraffin-embedded heart sections showed that atrial fibrotic remodeling was prevented in the mesalazine-treated PLK2 knockout mice (Figure 8G and 8H). This proof-of-concept study validated that inhibition of the ERK/OPN axis downstream of PLK2 is sufficient to prevent the profibrotic phenotype in PLK2 knockout mice.

DISCUSSION

In the present study, we demonstrate a novel role of PLK2 downregulation in fibroblast activation, subsequent myofibroblast differentiation, and enhanced OPN secretion, which contributes to the evolution of atrial fibrosis. The downregulation of PLK2 is accompanied by increased expression and secretion of OPN in patients with AF, and the loss of PLK2 in mice promotes de novo OPN secretion and cardiac fibrosis increasing the susceptibility to inducible AF. Accompanied by clear downregulation of PLK2 in atria of patients with AF, these results point to a novel and potentially important pathophysiological role in AF.

We demonstrate that PLK2 inhibition or knockout induce myofibroblast differentiation and reduce proliferation of cardiac fibroblasts, which is consistent with findings showing that PLK2 is a key regulator for proliferation and differentiation in cardiac progenitor cells.[12] Of note, PLK2 expression was much more abundant in primary atrial fibroblasts compared with primary atrial cardiomyocytes (Figure 1B). Primary human cardiac fibroblasts from patients with AF have reduced PLK2 levels, increased differentiation into myofibroblasts and a lower proliferation rate compared with SR controls.[11] Myofibroblasts are highly active secretory cells that substantially contribute to fibrosis in the diseased heart.[8,10,23] We noted substantial extracellular collagen deposition in vitro, interstitial fibrosis in the atria as well as ventricles in PLK2 knockout mice, which along with atrial dilation should create an arrhythmogenic substrate for AF maintenance. Indeed, we were able to induce AF-mimicking arrhythmias in 44% of PLK2 knockout mice but in none of the littermate controls. Our data identify reduced PLK2 expression as a novel molecular trigger of atrial fibrosis and AF promotion. PLK2 knockout mice had normal atrial action potentials and refractoriness (Figures II and IV in the Data Supplement). In addition, Ca^{2+} imaging experiments showed that neither PLK2 deficiency nor selective pharmacological inhibition of PLK2 affected cardiomyocyte Ca^{2+} handling and dynamics (Figure III in

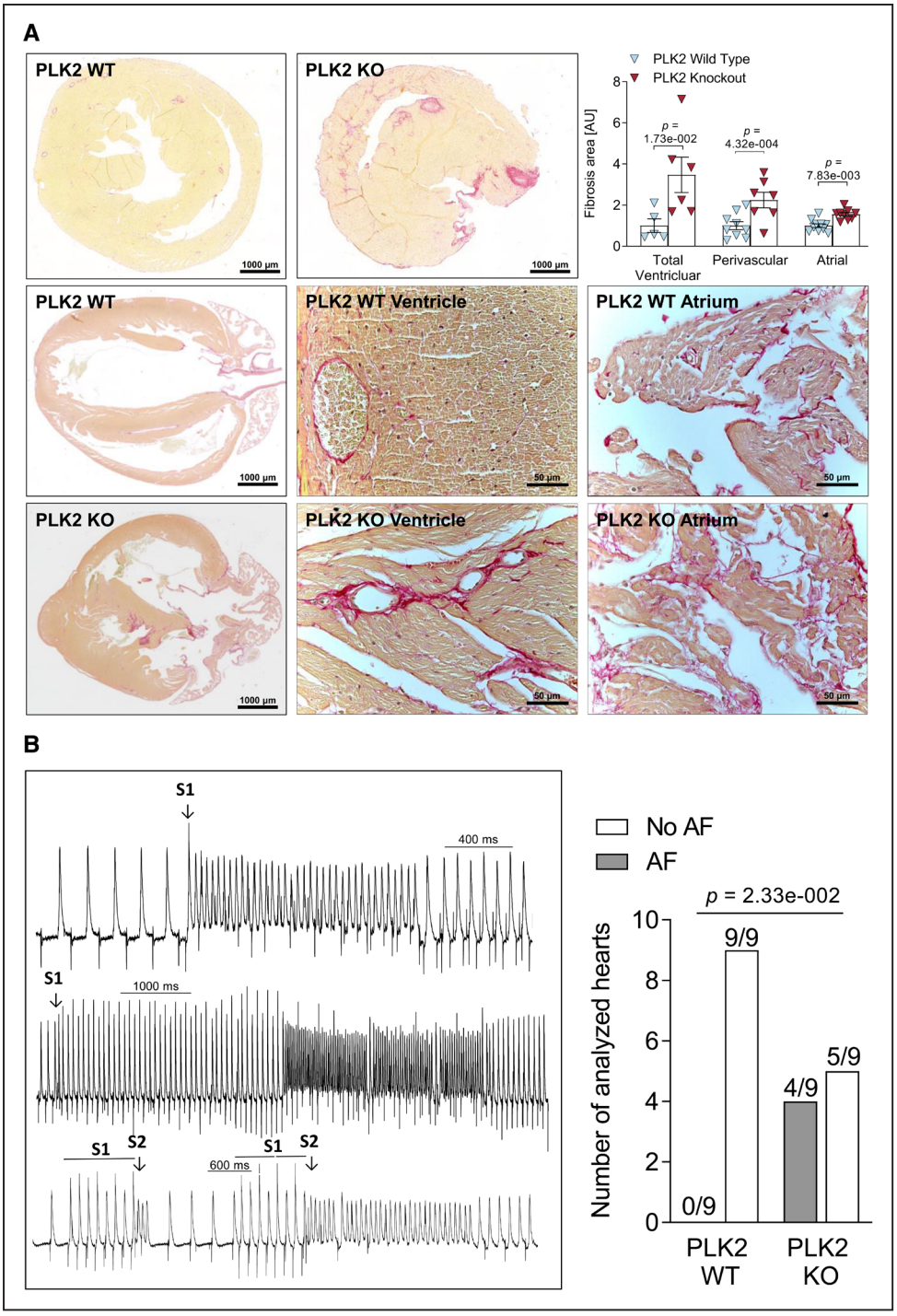

Figure 7. Loss of PLK2 (polo-like kinase 2) induces interstitial fibrosis and atrial fibrillation (AF) susceptibility.
A, Histological sections of murine hearts stained with Picrosirius red together with quantification of fibrosis. Microscopic pictures were taken along the short axis at mid-ventricular level (top) and the long axis (lower). The middle and right lower show magnifications of ventricular and atrial tissue, respectively ($WT_{Ventricular}$ [n=5], $KO_{Ventricular}$ [n=6], $WT_{Perivascular}$ [n=9], $KO_{Perivascular}$ [n=7], WT_{Atrial} [n=10], KO_{Atrial} [n=9]; right upper shows evaluation of one randomly selected slide per animal). Results are given as mean±SEM, *P* value was determined by a Mann-Whitney *U* test (for total ventricular fibrosis) and unpaired, 2-tailed *t* tests (for perivascular and atrial fibrosis). **B**, Representative monophasic action potentials recorded upon standard S1 and S1S2 stimulation protocols from the atrium of a Langendorff-perfused PLK2 KO heart (left). Numbers of AF-inducible vs noninducible atria (right) were analyzed by χ^2 test (WT [n=9], KO [n=9]). AU indicates arbitrary unit—red (fibrotic) area normalized to the total area of the respective section and to PLK2 WT control.

the Data Supplement), making altered atrial cardiomyocyte function an unlikely determinant of PLK2-dependent atrial arrhythmogenesis.

Probing for a mechanism of the downregulation of PLK2 in AF, we discovered PLK2 promotor methylation in 6 of 13 right atrial tissue samples from patients with

ORIGINAL RESEARCH

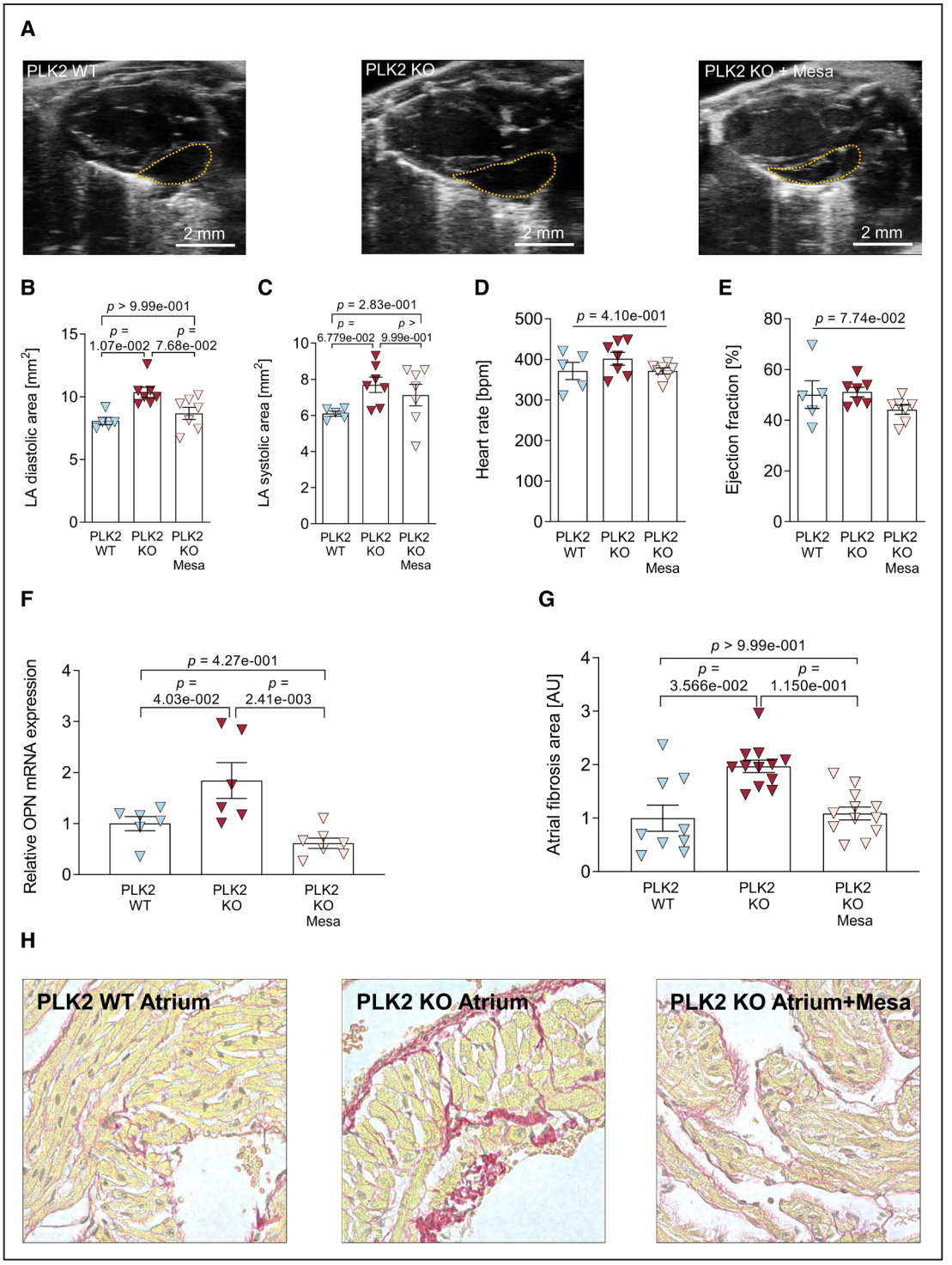

Figure 8. Pharmacological modulation of the ERK (extracellular-signal regulated kinases 1/2)-OPN (osteopontin)-axis with mesalazine. **A**, Representative parasternal long-axis views of native PLK2 (polo-like kinase 2) wild-type (WT) and knockout (KO) and mesalazine-treated KO animals. **B**, Left atrial diastolic area (WT [n=5], KO [n=7], KO+Mesa [n=7]; results are given as mean±SEM, *P* value was determined by a Kruskal-Wallis test with Dunn multiple comparisons test). **C**, Left atrial systolic area (WT [n=5], KO [n=7], KO+Mesa [n=7]; results are given as mean±SEM, *P* value was determined by a Kruskal-Wallis test with Dunn multiple comparisons test). **D**, Heart rate (WT [n=5], KO [n=7], KO+Mesa [n=7]; results are given as mean±SEM, *P* value was determined by a Kruskal-Wallis test with Dunn multiple comparisons test). **E**, Ejection fraction (WT [n=5], KO [n=7], KO+Mesa [n=7]; results are given as mean±SEM, *P* value was determined by a Kruskal-Wallis test with Dunn multiple comparisons test). **F**, Cardiac OPN gene expression normalized to HPRT as housekeeping gene (WT [n=6], KO [n=6], KO+Mesa [n=7]; results are given as mean±SEM, *P* value was determined by a 1-Way ANOVA with Tukey multiple comparisons test). **G** and **H**, Quantification of atrial fibrosis and representative histological sections (WT [n=9, N=3], KO [n=12, N=4], KO+Mesa [n=12, N=4]; results are given as mean±SEM). *P* value was determined by a hierarchical model using log-transformed data for normality reasons. AU indicates arbitrary unit—red (fibrotic) area normalized to the total area of the respective section and to PLK2 WT control.

AF, but in none of the patients with SR. We used hypoxia as a tool to induce PLK2 promotor methylation in vitro, since hypoxia has been shown to induce PLK2 promotor methylation in lymphocytes[27] and typically occurs during AF.[30,31] We observed pronounced PLK2 downregulation already after 24 hours of hypoxia treatment (1% O_2) with a discrepancy in the increase of *PLK2* promoter methylation not occurring before 4 days of hypoxia exposure. This is in line with findings showing 4 days of hypoxia as minimum threshold for the detection of DNA methylation in human fibroblasts.[42] However, a significant upregulation of the DNA-methylating enzymes DNMT1 and DNMT3A was already detectable after 24 hours of hypoxia (Figure 2E and 2F), pointing to presence of latent DNA methylation at early stages. This notion is further supported by the normalized PLK2 expression with the methylation inhibitor 5-azacytidine during hypoxia. Parallel to PLK2 downregulation, OPN expression was upregulated within 24 hours of hypoxia onset. After 96 hours of hypoxia exposure, OPN expression was nearly reverted to control levels (Figure 4F). This could either be because of cellular decay caused by prolonged hypoxia exposure or due to increased OPN degradation by MMP3 or MMP7 as a feedback regulation to oppose OPN.[43] Inhibition of ERK1/2 prevented OPN expression in PLK2 knockout atrial fibroblasts, mechanistically linking the suppression of PLK2 expression with the enhancement of OPN secretion. Interestingly, PLK1 has been shown to limit the ERK signaling pathway,[44] and ERK1/2 has previously been shown to modulate OPN transcription.[39,40,45] Overall, our results indicate that PLK2 ensures proper ERK1/2 function in cardiac fibroblasts and that loss of PLK2 function induces OPN secretion via increased ERK1/2 phosphorylation.

Myofibroblasts are known to secrete extracellular matrix proteins and inflammatory cytokines.[8,10,23] In PLK2 knockout fibroblast culture media, discovery proteomics revealed de novo secretion of OPN, which has been shown to promote fibrosis, remodeling, and cardiomyopathy.[15–23] In patients with AF, OPN was elevated on tissue-level in right atria as well as systemically in the peripheral blood of patients with low-voltage zones in comparison to SR controls. The plasma levels of OPN we found in patients with AF are in the range of 25 ng/mL, a concentration which increased myofibroblast differentiation in cultured fibroblasts. A recent publication on OPN levels in patients with AF also reported higher OPN levels, especially in patients with low-voltage zones.[46] Therefore, it is tempting to speculate that secreted OPN may serve as a systemic promoter of organ fibrosis. In fact, an association of AF with ventricular fibrosis has been reported.[47] Even higher OPN plasma levels (around 74 ng/mL) have been found in patients with advanced heart failure undergoing ICD implantation and were predictive for presence of ventricular tachycardia and fibrillation in this population.[48] Moreover, AF was diagnosed in some of these patients at the time of blood sampling. Overall, it appears that by causing fibrosis OPN could create an arrhythmogenic substrate for arrhythmias other than AF.

Finally, to validate our findings and to test for therapeutic potential, we performed a proof-of-concept study by pharmacologically targeting the pathological profibrotic PLK2 knockout phenotype. As selective PLK2 activators are not available, yet, we chose oral application of mesalazine. In a rodent preclinical model of liver fibrosis, this drug showed strong antifibrotic effects by a reduction of OPN expression.[41] Our previous data similarly showed that mesalazine has significant antifibrotic effects mainly mediated by inhibition of ERK-phosphorylation in an in vitro model of cardiac fibrosis.[24] Here, we provide a proof-of-concept that long-term treatment with mesalazine reverses the PLK2 knockout phenotype by normalizing cardiac OPN expression and preventing atrial fibrosis and dilatation (Figure 8). Thus, mesalazine may serve as a lead compound for the development of selective modulators of the ERK/OPN axis that target AF-promoting atrial fibrosis.

Potential Limitations

For the clinical substrate assessment in patients with AF, high-density mapping catheters and cardiac magnetic resonance imaging should ideally be combined. Thus, the absence of magnetic resonance imaging validation should be considered when interpreting our high-density mapping results. Although atrial dilatation is considered as a clinical determinant of AF, left atrial volume is a better predictor of AF and its recurrence rate.[49] We matched our patients as much as possible about age, sex, comorbidities, and medication, but the associated extraneous sources of variance can never be completely eliminated. The effect of PLK2 reduction in human AF is likely less than in the PLK2 knockout mouse, since in human AF the reduction in PLK2 mRNA abundance is only ≈50%. We also cannot rule out a contribution of alterations in diastolic function to the PLK2 knockout phenotype. Moreover, we did not assess cellular coupling and therefore cannot exclude alterations in conduction velocity induced by remodeling of connexins. Correction for multiple testing was performed for each individual test as indicated. We did however not correct for multiple testing across the entire work. This should be considered in interpreting our statistical analyses and constitutes a potential weakness of the study.

Nevertheless, studies using human cardiac tissues provide valuable information on clinical relevance particularly when used in conjunction with studies in animal models to address specific hypotheses and study cause-effect relationships as we did in the present work.

CONCLUSIONS

The present study demonstrates that the PLK2-OPN axis in atrial fibroblasts contributes to fibroblast dysfunction and the creation of AF-promoting atrial fibrosis. To our knowledge, this is the first study to propose a pathological role for the family of polo-like kinases in AF pathophysiology. We provide a mechanistic link between reduced PLK2 expression in AF and increased OPN release and show that PLK2 downregulation is sufficient to cause fibrosis thereby increasing the susceptibility to induce AF in mouse hearts. Chronic treatment with mesalazine effectively prevented the profibrotic PLK2 knockout phenotype, thus providing of proof-of-concept for therapeutic targeting of the OPN/ERK axis. This may constitute a novel antifibrotic approach to prevent atrial fibrosis and to halt the progression to therapy-resistant persistent forms of AF.

ARTICLE INFORMATION

Received May 3, 2021; revision received August 24, 2021; accepted August 25, 2021.

Affiliations

Institute of Pharmacology and Toxicology, Faculty of Medicine Carl Gustav Carus, Technische Universität Dresden (S.R.K., M.H., S.W., K.K., S.K., M.G., E.K., J.S.E.R., M.S.S., T.K., S.M.-R., K.G., M.W., A.E.-A.). Department of Rhythmology (C.P., M.W.) and Department of Cardiac Surgery (S.M.T.), Clinic for Internal Medicine and Cardiology, Heart Center Dresden GmbH, Dresden, Technische Universität Dresden. Unit for Degradomics of the Protease Web, Institute of Biochemistry, University of Kiel (S.R.-J.). The James Black Centre, King's College, University of London (X.Y., M.M.). Department of Gynecology and Obstetrics, Medical Faculty and University Hospital Carl Gustav Carus, Technische Universität Dresden (J.D.K., P.W.). German Cancer Consortium (DKTK), Dresden and German Cancer Research Center (DKFZ), Heidelberg (J.D.K., P.W.). National Center for Tumor Diseases (NCT), Partner Site Dresden (J.D.K., P.W., K.G.). Brandenburg University of Technology, Senftenberg (N.H., J.-H.K.). Institute of Cardiovascular Sciences, University of Birmingham (M.O., S.N.K., L.C.S.). Institute of Clinical Chemistry and Laboratory Medicine, Technische Universität Dresden (B.W.). Department of Cardiology, University Hospitals Birmingham (L.F.). Department of Medicine, Montreal Heart Institute and Université de Montréal, Quebec, Canada (S.N., D.D.). Institut für Experimentelle Kardiovaskuläre Medizin, Universitäts Herzzentrum, Freiburg Bad Krotzingen, Freiburg im Breisgau (U.R.). Institute of Pharmacology, West German Heart and Vascular Center, University Duisburg-Essen (S.N., D.D.). IHU Liryc, Electrophysiology and Heart Modeling Institute, Fondation Bordeaux Université (S.N.). Department of Molecular Physiology and Biophysics, Baylor College of Medicine (D.D.). Department of Dermatology, Faculty of Medicine Carl Gustav Carus, Technische Universität Dresden (S.R.K.). Internal Medicine III, University Hospital Carl Gustav Carus, Technische Universität Dresden (M.M.). University Center of Cardiovascular Science and Department of Cardiology, University Heart and Vascular Center Hamburg (L.F., L.C.S.).

Acknowledgments

We are grateful to Manja Newe, Annett Opitz, Romy Kempe, Andreas Schwab, and Stephanie M. Schacht-Wall for expert technical assistance.

Author Contributions

S.R. Künzel designed and performed the experiments, analyzed the data, prepared the figures, and wrote the article. M. Hoffmann conducted experiments and wrote the article. S. Weber designed experiments and contributed to the article preparation. K. Künzel designed and performed experiments and analyzed data. E. Klapproth, J.S.E. Rausch, M.S. Sadek, M. Günscht, and T. Kolanowski contributed to the article preparation. S. Meyer-Roxlau supervised the animal work. C. Piorkowski provided clinical data and blood samples. S.M. Tugtekin provided primary human heart tissue samples for subsequent cell cultures. S. Rose-John provided the PLK2 knockout animals and expert knowledge. M. Mayr designed experiments and provided support for the mass spectrometry. X. Yin performed experiments and provided support for the analysis of mass spectrometry data. J. Dominik Kuhlmann, P. Wimberger, and K. Grützmann designed and performed experiments and contributed to article preparation. N. Herzog and J.-H. Küpper contributed to article preparation. S.N. Kabir, M. O'Reilly, and L.C. Sommerfeld performed and analyzed atrial pacing and electrophysiological measurements in the isolated heart supervised by L. Fabritz, U. Ravens, S. Kämmerer. B. Wielockx, D. Dobrev, and K. Guan supervised the experiments, helped with article preparation, and critically reviewed the article. S. Nattel provided the ventricular tachypacing samples, supervised the experiments and critically reviewed the article. M. Wagner and A. El-Armouche supervised the work and wrote the article.

Sources of Funding

This work was supported by grants from the DFG (German Research Foundation) within the CRC/Transregio 205/2 to B. Wielockx and A. El-Armouche (A02), DFG grant EL 270/7-3 to A. El-Armouche, the DFG IRTG 2251 to A. El-Armouche and S. Kämmerer. (D11) and DFG grant WA 2586/4-1 to M. Wagner. This work was supported by a "MeDDrive Start" grant of the Faculty of Medicine Carl Gustav Carus, Dresden (to S.R. Künzel). The Institute of Cardiovascular Research, University of Birmingham, has received an Accelerator Award by the British Heart Foundation AA/18/2/34218. D. Dobrev and L. Fabritz received an EU Horizon 2020 MAESTRIA grant (965286).

Disclosures

All authors concur with the submission of the article and none of the data have been previously reported or are under consideration for publication elsewhere. Parts of doctoral theses of S.R. Künzel, M. Hoffmann, and J.S.E. Rausch are included in this article. The other authors report no conflicts.

Supplemental Materials

Expanded Materials & Methods
Data Supplement Figures I–V
Data Supplement Tables I–XIV
References[50–58]
Major Resources Table

REFERENCES

1. Chung MK, Refaat M, Shen WK, Kutyifa V, Cha YM, Di Biase L, Baranchuk A, Lampert R, Natale A, Fisher J, et al; ACC Electrophysiology Section Leadership Council. Atrial fibrillation: JACC Council Perspectives. *J Am Coll Cardiol*. 2020;75:1689–1713. doi: 10.1016/j.jacc.2020.02.025
2. Harada M, Van Wagoner DR, Nattel S. Role of inflammation in atrial fibrillation pathophysiology and management. *Circ J*. 2015;79:495–502. doi: 10.1253/circj.CJ-15-0138
3. Hadi HA, Alsheikh-Ali AA, Mahmeed WA, Suwaidi JM. Inflammatory cytokines and atrial fibrillation: current and prospective views. *J Inflamm Res*. 2010;3:75–97. doi: 10.2147/JIR.S10095
4. Boos CJ, Anderson RA, Lip GY. Is atrial fibrillation an inflammatory disorder? *Eur Heart J*. 2006;27:136–149. doi: 10.1093/eurheartj/ehi645
5. Dan GA, Dobrev D. Antiarrhythmic drugs for atrial fibrillation: imminent impulses are emerging. *Int J Cardiol Heart Vasc*. 2018;21:11–15. doi: 10.1016/j.ijcha.2018.08.005
6. Heijman J, Guichard JB, Dobrev D, Nattel S. Translational challenges in atrial fibrillation. *Circ Res*. 2018;122:752–773. doi: 10.1161/CIRCRESAHA.117.311081
7. Goette A, Kalman JM, Aguinaga L, Akar J, Cabrera JA, Chen SA, Chugh SS, Corradi D, D'Avila A, Dobrev D, et al; Document Reviewers. EHRA/HRS/APHRS/SOLAECE expert consensus on atrial cardiomyopathies: definition, characterization, and clinical implication. *Europace*. 2016;18:1455–1490. doi: 10.1093/europace/euw161
8. Tallquist MD, Molkentin JD. Redefining the identity of cardiac fibroblasts. *Nat Rev Cardiol*. 2017;14:484–491. doi: 10.1038/nrcardio.2017.57
9. Nattel S, Burstein B, Dobrev D. Atrial remodeling and atrial fibrillation: mechanisms and implications. *Circ Arrhythm Electrophysiol*. 2008;1:62–73. doi: 10.1161/CIRCEP.107.754564
10. Baum J, Duffy HS. Fibroblasts and myofibroblasts: what are we talking about? *J Cardiovasc Pharmacol*. 2011;57:376–379. doi: 10.1097/FJC.0b013e3182116e39
11. Poulet C, Künzel S, Büttner E, Lindner D, Westermann D, Ravens U. Altered physiological functions and ion currents in atrial fibroblasts from patients with chronic atrial fibrillation. *Physiol Rep*. 2016;4:e12681. doi: 10.14814/phy2.12681
12. Mochizuki M, Lorenz V, Ivanek R, Della Verde G, Gaudiello E, Marsano A, Pfister O, Kuster GM. Polo-Like Kinase 2 is dynamically regulated to

coordinate proliferation and early lineage specification downstream of Yes-Associated Protein 1 in cardiac progenitor cells. *J Am Heart Assoc*. 2017;6:e005920. doi: 10.1161/JAHA.117.005920
13. Li J, Ma W, Wang PY, Hurley PJ, Bunz F, Hwang PM. Polo-like kinase 2 activates an antioxidant pathway to promote the survival of cells with mitochondrial dysfunction. *Free Radic Biol Med*. 2014;73:270–277. doi: 10.1016/j.freeradbiomed.2014.05.022
14. Ma S, Charron J, Erikson RL. Role of Plk2 (Snk) in mouse development and cell proliferation. *Mol Cell Biol*. 2003;23:6936–6943. doi: 10.1128/MCB.23.19.6936-6943.2003
15. López B, González A, Lindner D, Westermann D, Ravassa S, Beaumont J, Gallego I, Zudaire A, Brugnolaro C, Querejeta R, et al. Osteopontin-mediated myocardial fibrosis in heart failure: a role for lysyl oxidase? *Cardiovasc Res*. 2013;99:111–120. doi: 10.1093/cvr/cvt100
16. Rubiś P, Wiśniowska-Śmiałek S, Dziewięcka E, Rudnicka-Sosin L, Kozanecki A, Podolec P. Prognostic value of fibrosis-related markers in dilated cardiomyopathy: a link between osteopontin and cardiovascular events. *Adv Med Sci*. 2018;63:160–166. doi: 10.1016/j.advms.2017.10.004
17. Lenga Y, Koh A, Perera AS, McCulloch CA, Sodek J, Zohar R. Osteopontin expression is required for myofibroblast differentiation. *Circ Res*. 2008;102:319–327. doi: 10.1161/CIRCRESAHA.107.160408
18. Herum KM, Romaine A, Wang A, Melleby AO, Strand ME, Pacheco J, Braathen B, Dunér P, Tønnessen T, Lunde IG, et al. Syndecan-4 protects the heart from the profibrotic effects of thrombin-cleaved osteopontin. *J Am Heart Assoc*. 2020;9:e013518. doi: 10.1161/JAHA.119.013518
19. Singh K, Sirokman G, Communal C, Robinson KG, Conrad CH, Brooks WW, Bing OH, Colucci WS. Myocardial osteopontin expression coincides with the development of heart failure. *Hypertension*. 1999;33:663–670. doi: 10.1161/01.hyp.33.2.663
20. Trueblood NA, Xie Z, Communal C, Sam F, Ngoy S, Liaw L, Jenkins AW, Wang J, Sawyer DB, Bing OH, et al. Exaggerated left ventricular dilation and reduced collagen deposition after myocardial infarction in mice lacking osteopontin. *Circ Res*. 2001;88:1080–1087. doi: 10.1161/hh1001.090842
21. Xie Z, Singh M, Singh K. Osteopontin modulates myocardial hypertrophy in response to chronic pressure overload in mice. *Hypertension*. 2004;44:826–831. doi: 10.1161/01.HYP.0000148458.03202.48
22. Sam F, Xie Z, Ooi H, Kerstetter DL, Colucci WS, Singh M, Singh K. Mice lacking osteopontin exhibit increased left ventricular dilation and reduced fibrosis after aldosterone infusion. *Am J Hypertens*. 2004;17:188–193. doi: 10.1016/j.amjhyper.2003.10.007
23. Frangogiannis NG. Matricellular proteins in cardiac adaptation and disease. *Physiol Rev*. 2012;92:635–688. doi: 10.1152/physrev.00008.2011
24. Hoffmann M, Kant TA, Emig R, Rausch JSE, Newe M, Schubert M, Künzel K, Winter L, Klapproth E, Peyronnet R, et al. Repurposing mesalazine against cardiac fibrosis in vitro. *Naunyn Schmiedebergs Arch Pharmacol*. 2021;394:533–543. doi: 10.1007/s00210-020-01998-9
25. Sikkel MB, Francis DP, Howard J, Gordon F, Rowlands C, Peters NS, Lyon AR, Harding SE, MacLeod KT. Hierarchical statistical techniques are necessary to draw reliable conclusions from analysis of isolated cardiomyocyte studies. *Cardiovasc Res*. 2017;113:1743–1752. doi: 10.1093/cvr/cvx151
26. Li D, Fareh S, Leung TK, Nattel S. Promotion of atrial fibrillation by heart failure in dogs: atrial remodeling of a different sort. *Circulation*. 1999;100:87–95. doi: 10.1161/01.cir.100.1.87
27. Syed N, Smith P, Sullivan A, Spender LC, Dyer M, Karran L, O'Nions J, Allday M, Hoffmann I, Crawford D, et al. Transcriptional silencing of Polo-like kinase 2 (SNK/PLK2) is a frequent event in B-cell malignancies. *Blood*. 2006;107:250–256. doi: 10.1182/blood-2005-03-1194
28. Benetatos L, Dasoula A, Hatzimichael E, Syed N, Voukelatou M, Dranitsaris G, Bourantas KL, Crook T. Polo-Like Kinase 2 (SNK/PLK2) is a novel epigenetically regulated gene in acute myeloid leukemia and myelodysplastic syndromes: genetic and epigenetic interactions. *Ann Hematol*. 2011;90:1037–1045. doi: 10.1007/s00277-011-1193-4
29. Künzel SR, Rausch JSE, Schäffer C, Hoffmann M, Künzel K, Klapproth E, Kant T, Herzog N, Küpper JH, Lorenz K, et al. Modeling atrial fibrosis in vitro-generation and characterization of a novel human atrial fibroblast cell line. *FEBS Open Bio*. 2020;10:1210–1218. doi: 10.1002/2211-5463.12896
30. Gramley F, Lorenzen J, Jedamzik B, Gatter K, Koellensperger E, Munzel T, Pezzella F. Atrial fibrillation is associated with cardiac hypoxia. *Cardiovasc Pathol*. 2010;19:102–111. doi: 10.1016/j.carpath.2008.11.001
31. Opacic D, van Bragt KA, Nasrallah HM, Schotten U, Verheule S. Atrial metabolism and tissue perfusion as determinants of electrical and structural remodelling in atrial fibrillation. *Cardiovasc Res*. 2016;109:527–541. doi: 10.1093/cvr/cvw007
32. Ayrapetov MK, Xu C, Sun Y, Zhu K, Parmar K, D'Andrea AD, Price BD. Activation of Hif1α by the prolylhydroxylase inhibitor dimethyoxalyglycine decreases radiosensitivity. *PLoS One*. 2011;6:e26064. doi: 10.1371/journal.pone.0026064
33. Okano M, Bell DW, Haber DA, Li E. DNA methyltransferases Dnmt3a and Dnmt3b are essential for de novo methylation and mammalian development. *Cell*. 1999;99:247–257. doi: 10.1016/s0092-8674(00)81656-6
34. Christman JK. 5-Azacytidine and 5-aza-2'-deoxycytidine as inhibitors of DNA methylation: mechanistic studies and their implications for cancer therapy. *Oncogene*. 2002;21:5483–5495. doi: 10.1038/sj.onc.1205699
35. Inglis KJ, Chereau D, Brigham EF, Chiou SS, Schöbel S, Frigon NL, Yu M, Caccavello RJ, Nelson S, Motter R, et al. Polo-Like Kinase 2 (PLK2) phosphorylates alpha-synuclein at serine 129 in central nervous system. *J Biol Chem*. 2009;284:2598–2602. doi: 10.1074/jbc.C800206200
36. Coppé JP, Patil CK, Rodier F, Sun Y, Muñoz DP, Goldstein J, Nelson PS, Desprez PY, Campisi J. Senescence-associated secretory phenotypes reveal cell-nonautonomous functions of oncogenic RAS and the p53 tumor suppressor. *PLoS Biol*. 2008;6:2853–2868. doi: 10.1371/journal.pbio.0060301
37. Verma A, Wazni OM, Marrouche NF, Martin DO, Kilicaslan F, Minor S, Schweikert RA, Saliba W, Cummings J, Burkhardt JD, et al. Pre-existent left atrial scarring in patients undergoing pulmonary vein antrum isolation: an independent predictor of procedural failure. *J Am Coll Cardiol*. 2005;45:285–292. doi: 10.1016/j.jacc.2004.10.035
38. Huo Y, Gaspar T, Pohl M, Sitzy J, Richter U, Neudeck S, Mayer J, Kronborg MB, Piorkowski C. Prevalence and predictors of low voltage zones in the left atrium in patients with atrial fibrillation. *Europace*. 2018;20:956–962. doi: 10.1093/europace/eux082
39. Hickey FB, England K, Cotter TG. Bcr-Abl regulates osteopontin transcription via Ras, PI-3K, aPKC, Raf-1, and MEK. *J Leukoc Biol*. 2005;78:289–300. doi: 10.1189/jlb.1104655
40. El-Tanani MK, Campbell FC, Kurisetty V, Jin D, McCann M, Rudland PS. The regulation and role of osteopontin in malignant transformation and cancer. *Cytokine Growth Factor Rev*. 2006;17:463–474. doi: 10.1016/j.cytogfr.2006.09.010
41. Ramadan A, Afifi N, Yassin NZ, Abdel-Rahman RF, Abd El-Rahman SS, Fayed HM. Mesalazine, an osteopontin inhibitor: the potential prophylactic and remedial roles in induced liver fibrosis in rats. *Chem Biol Interact*. 2018;289:109–118. doi: 10.1016/j.cbi.2018.05.002
42. Robinson CM, Neary R, Levendale A, Watson CJ, Baugh JA. Hypoxia-induced DNA hypermethylation in human pulmonary fibroblasts is associated with Thy-1 promoter methylation and the development of a pro-fibrotic phenotype. *Respir Res*. 2012;13:74. doi: 10.1186/1465-9921-13-74
43. Agnihotri R, Crawford HC, Haro H, Matrisian LM, Havrda MC, Liaw L. Osteopontin, a novel substrate for matrix metalloproteinase-3 (stromelysin-1) and matrix metalloproteinase-7 (matrilysin). *J Biol Chem*. 2001;276:28261–28267. doi: 10.1074/jbc.M103608200
44. Li R, Chen DF, Zhou R, Jia SN, Yang JS, Clegg JS, Yang WJ. Involvement of polo-like kinase 1 (Plk1) in mitotic arrest by inhibition of mitogen-activated protein kinase-extracellular signal-regulated kinase-ribosomal S6 kinase 1 (MEK-ERK-RSK1) cascade. *J Biol Chem*. 2012;287:15923–15934. doi: 10.1074/jbc.M111.312413
45. Xie Z, Singh M, Singh K. ERK1/2 and JNKs, but not p38 kinase, are involved in reactive oxygen species-mediated induction of osteopontin gene expression by angiotensin II and interleukin-1beta in adult rat cardiac fibroblasts. *J Cell Physiol*. 2004;198:399–407. doi: 10.1002/jcp.10419
46. Lin R, Wu S, Zhu D, Qin M, Liu X. Osteopontin induces atrial fibrosis by activating Akt/GSK-3β/β-catenin pathway and suppressing autophagy. *Life Sci*. 2020;245:117328. doi: 10.1016/j.lfs.2020.117328
47. Dzeshka MS, Lip GY, Snezhitskiy V, Shantsila E. Cardiac fibrosis in patients with atrial fibrillation: mechanisms and clinical implications. *J Am Coll Cardiol*. 2015;66:943–959. doi: 10.1016/j.jacc.2015.06.1313
48. Francia P, Adduci C, Semprini L, Borro M, Ricotta A, Sensini I, Santini D, Caprinozzi M, Balla C, Simmaco M, et al. Osteopontin and galectin-3 predict the risk of ventricular tachycardia and fibrillation in heart failure patients with implantable defibrillators. *J Cardiovasc Electrophysiol*. 2014;25:609–616. doi: 10.1111/jce.12364
49. Njoku A, Kannabhiran M, Arora R, Reddy P, Gopinathannair R, Lakkireddy D, Dominic P. Left atrial volume predicts atrial fibrillation recurrence after radiofrequency ablation: a meta-analysis. *Europace*. 2018;20:33–42. doi: 10.1093/europace/eux013
50. Huo Y, Christoph M, Forkmann M, Pohl M, Mayer J, Salmas J, Sitzy J, Wunderlich C, Piorkowski C, Gaspar T. Reduction of radiation exposure during atrial fibrillation ablation using a novel fluoroscopy image integrated 3-dimensional electroanatomic mapping system: a prospective, randomized, single-blind, and controlled study. *Heart Rhythm*. 2015;12:1945–1955. doi: 10.1016/j.hrthm.2015.05.018

51. El-Armouche A, Wittköpper K, Degenhardt F, Weinberger F, Didié M, Melnychenko I, Grimm M, Peeck M, Zimmermann WH, Unsöld B, et al. Phosphatase inhibitor-1-deficient mice are protected from catecholamine-induced arrhythmias and myocardial hypertrophy. *Cardiovasc Res*. 2008;80:396–406. doi: 10.1093/cvr/cvn208
52. Kant TA, Newe M, Winter L, Hoffmann M, Kämmerer S, Klapproth E, Künzel K, Kühnel MP, Neubert L, El-Armouche A, et al. Genetic deletion of polo-like kinase 2 induces a pro-fibrotic pulmonary phenotype. *Cells*. 2021;10:617. doi: 10.3390/cells10030617
53. Yin X, Bern M, Xing Q, Ho J, Viner R, Mayr M. Glycoproteomic analysis of the secretome of human endothelial cells. *Mol Cell Proteomics*. 2013;12:956–978. doi: 10.1074/mcp.M112.024018
54. Abonnenc M, Nabeebaccus AA, Mayr U, Barallobre-Barreiro J, Dong X, Cuello F, Sur S, Drozdov I, Langley SR, Lu R, et al. Extracellular matrix secretion by cardiac fibroblasts: role of microRNA-29b and microRNA-30c. *Circ Res*. 2013;113:1138–1147. doi: 10.1161/CIRCRESAHA.113.302400
55. Vettel C, Lindner M, Dewenter M, Lorenz K, Schanbacher C, Riedel M, Lämmle S, Meinecke S, Mason FE, Sossalla S, et al. Phosphodiesterase 2 protects against catecholamine-induced arrhythmia and preserves contractile function after myocardial infarction. *Circ Res*. 2017;120:120–132. doi: 10.1161/CIRCRESAHA.116.310069
56. Syeda F, Holmes AP, Yu TY, Tull S, Kuhlmann SM, Pavlovic D, Betney D, Riley G, Kucera JP, Jousset F, et al. PITX2 modulates atrial membrane potential and the antiarrhythmic effects of sodium-channel blockers. *J Am Coll Cardiol*. 2016;68:1881–1894. doi: 10.1016/j.jacc.2016.07.766
57. Blana A, Kaese S, Fortmüller L, Laakmann S, Damke D, van Bragt K, Eckstein J, Piccini I, Kirchhefer U, Nattel S, et al. Knock-in gain-of-function sodium channel mutation prolongs atrial action potentials and alters atrial vulnerability. *Heart Rhythm*. 2010;7:1862–1869. doi: 10.1016/j.hrthm.2010.08.016
58. Obergassel J, O'Reilly M, Sommerfeld LC, Kabir SN, O'Shea C, Syeda F, Eckardt L, Kirchhof P, Fabritz L. Effects of genetic background, sex, and age on murine atrial electrophysiology. *Europace*. 2021;23:958–969. doi: 10.1093/europace/euaa369